

NO EVIDENCE OF CIRCUMSTELLAR GAS SURROUNDING TYPE IA SUPERNOVA SN 2017cbv

RAPHAEL FERRETTI,¹ RAHMAN AMANULLAH,¹ MATTIA BULLA,¹ ARIEL GOOBAR,¹ JOEL JOHANSSON,^{2,3} AND
PETER LUNDQVIST⁴

¹*Oskar Klein Centre, Department of Physics, Stockholm University, Albanova, SE 106 91 Stockholm, Sweden*

²*Benozio Center for Astrophysics, Weizmann Institute of Science, 76100 Rehovot, Israel*

³*Department of Physics and Astronomy, Division of Astronomy and Space Physics, Uppsala University, Box 516, SE 751 20 Uppsala, Sweden*

⁴*Oskar Klein Centre, Department of Astronomy, Stockholm University, Albanova, SE 106 91 Stockholm, Sweden*

(Received; Revised; Accepted)

Submitted to ApJL

ABSTRACT

Nearby type Ia supernovae (SNe Ia), such as SN 2017cbv, are useful events to address the question of what the elusive progenitor systems of the explosions are. Hosseinzadeh et al. (2017a) suggested that the early blue excess of the lightcurve of SN 2017cbv could be due to the supernova ejecta interacting with a nondegenerate companion star. Different SN Ia progenitor models are predicted to have circumstellar (CS) environments in which strong outflows create low density cavities of different radii. Matter deposited at the edges of the cavities, should be at distances at which photoionisation due to early ultraviolet (UV) radiation of SNe Ia causes detectable changes to the observable Na I D and Ca II H&K absorption lines. To study narrow absorption lines, we obtained a time-series of high-resolution spectra of SN 2017cbv at phases between -14.8 and $+83$ days with respect to B -band maximum, covering the time at which photoionisation is predicted to occur. Both narrow Na I D and Ca II H&K are detected in all spectra, without there being any measurable changes between the epochs. Photoionisation models suggest that no detectable gas clouds were present between $\sim 10^{15}$ – 2×10^{19} cm from SN 2017cbv. The limits exclude the presence of significant amounts of Na I and Ca II gas at distances some progenitor models suggest CS gas would be deposited.

Keywords: supernovae: individual (SN 2017cbv)

arXiv:1708.05394v1 [astro-ph.SR] 17 Aug 2017

1. INTRODUCTION

Due to their standard candle properties, type Ia supernovae (SNe Ia) are of great importance to modern cosmology (see e.g. [Goobar & Leibundgut 2011](#), for a review). Although they have been studied in great detail, with thousands of observed objects, the physics of the progenitor system leading to the explosion is still not fully understood. There exist two prevalent progenitor models for SNe Ia, both of which have observational evidence. The models involve the thermonuclear explosion of a carbon-oxygen (C/O) white dwarf in a binary system with another star, which it merges with or accretes mass from. If the companion star is another white dwarf, the system is referred to as a double degenerate (DD, [Iben & Tutukov 1984](#); [Webbink 1984](#)), and if it is a main sequence or giant star, a single degenerate progenitor (SD, [Whelan & Iben 1973](#)). More complicated systems, such as common envelope (or symbiotic) binaries ([Dilday et al. 2012](#)), and colliding white dwarfs have also been proposed ([Dong et al. 2015](#)).

The circumstellar (CS) environment of SNe Ia should hold clues to the progenitor systems. SD progenitors for instance are believed to have strong outflows, which excavate low density cavities into the surrounding interstellar medium (ISM) and deposit matter at the edges ([Badenes et al. 2007](#)). Similarly, models of DD Helium+C/O binary systems suggest there should be cavities with smaller radii ([Shen et al. 2013](#)). On much smaller scales, tidal effects in DD progenitors can deposit matter into the CS medium ([Raskin & Kasen 2013](#)).

Strong upper limits on outflowing matter have been set with radio ([Chomiuk et al. 2016](#); [Kundu et al. 2017](#)) and X-ray ([Margutti et al. 2014](#)) observations of individual SNe. Furthermore, the lack of thermal emission in mid- and far-infrared, has set strong limits on CS dust surrounding individual SNe Ia ([Johansson et al. 2013, 2017](#)). Nevertheless, there are observations, such as predominately blueshifted profiles of narrow Na I D absorption lines which suggest there is outflowing material somewhere along the lines-of-sight ([Sternberg et al. 2011](#); [Maguire et al. 2013](#)). The blueshifted profiles and frequently observed large Na I column densities ([Phillips et al. 2013](#)), could however also be explained by ISM dust grain collisions induced by SN radiation pressure ([Hoang 2017](#)).

Along with a recent method, which follows variable reddening of SNe Ia ([Bulla et al. 2017](#)), variations in narrow absorption line profiles can be used to locate gas close to SNe Ia. Before maximum brightness, photoionisation of gas close to the SNe should occur ([Borkowski et al. 2009](#)), leading to a decrease or disappearance of

characteristic absorption lines. At later phases recombination of the same gas could lead to the reappearance and increase in the same absorption lines. The distance of an absorber to the SN can be determined by recording the changes in absorption line profiles due to photoionisation. However, geometric effects ([Patat et al. 2010](#)) and changing levels of foreground light ([Maeda et al. 2016](#)) can also lead to variations.

A small number of SNe Ia with variable absorption lines have been observed to date:

- SN 2006X ([Patat et al. 2007](#)) showed a changing Na I D profile at late times. Although initially pointing to recombination, [Chugai \(2008\)](#) suggested a geometric origin of the variations.
- SN 2007le ([Simon et al. 2009](#)) also showed an increasing Na I D component.
- SN 2011fe ([Patat et al. 2013](#)) showed slight variations, consistent with geometric effects.
- PTF11kx ([Dilday et al. 2012](#)) showed many variable absorption features. The SN was peculiar and believed to have had a symbiotic progenitor.
- SN 2013gh ([Ferretti et al. 2016](#)) had a small varying Na I D component consistent with photoionisation or geometric effects.
- SN 2014J ([Graham et al. 2015](#)) showed a varying K I line while Na I D remained unchanged, which is consistent with photoionisation. [Maeda et al. \(2016\)](#) argue that the gas is unlikely to have been CS matter.

Notably, most of the above examples (except for SN 2011fe and the unusual PTF11kx) occurred in crowded fields with visible dust lanes along the lines-of-sight, where geometric effects cannot be excluded as the origin of the variations. A larger sample of 14 SNe Ia with multi-epoch high-resolution spectra ([Sternberg et al. 2014](#)), as well as other individual cases (e.g. [Amanullah et al. 2015](#); [Ferretti et al. 2016](#)), did not reveal further examples of varying absorption lines. However, almost all existing time-series of SNe Ia are taken at too late phases to probe for photoionisation of CS gas (as explained in [Ferretti et al. 2016](#)).

Because of its low redshift, early discovery and a line-of-sight seemingly clear of an ISM, the recently discovered SN Ia SN 2017cbv ([Hosseinzadeh et al. 2017a](#)) presents a good opportunity to search for photoionisation of CS gases. Below we present the time-series of high-resolution spectra we obtained of this object (Section 2), in which we identify narrow Na I D and

Ca II H&K absorption features and search for variations in them (Section 3). Finally, we compare our observations to the findings of Hosseinzadeh et al. (2017a) and conclude (Section 4 & 5).

2. OBSERVATIONS

SN 2017cbv was discovered on March 10 UT (MJD 57822.14) by the Distance Less Than 40 Mpc (DLT40) nearby SN survey (Tartaglia et al. 2017) and subsequently classified as a young SN Ia (Hosseinzadeh et al. 2017b). The SN is located in the outskirts of NGC 5643 at $z = 0.004$ (Koribalski et al. 2004), at $\alpha = 14^h 32^m 34^s.42$, $\delta = -44^\circ 57' 35''$ (J2000), a line-of-sight with galactic extinction $E(B - V)_{MW} = 0.15$ mag (Schlafly & Finkbeiner 2011). Lightcurve analysis by Hosseinzadeh et al. (2017a) determined that SN 2017cbv peaked at MJD 57841.07 in B -band with $\Delta m_{15}(B) = 1.06$ mag.

Due to its proximity, early discovery and a line-of-sight with little to no host galaxy ISM, SN 2017cbv was a good candidate to search for CS gas with high-resolution spectroscopy. For this purpose we triggered our ESO TOOs 098.A-0783(A) and 098.A-0783(B) (P.I. Amanullah) to obtain a time-series of high-resolution spectra with the Ultraviolet and Visual Echelle Spectrograph (UVES; Dekker et al. 2000) on Kueyen (UT2) at the Very Large Telescope (VLT). We reduced the spectra using the REFLEX (ESOREX) reduction pipeline provided by ESO (Modigliani et al. 2010) and use the telluric line correction software Molecfit (Smette et al. 2015; Kausch et al. 2015) where necessary. The obtained spectra are summarised in Table 1.

We obtained the first UVES spectrum on MJD 57826.3, 4.2 days after discovery, at an epoch of -14.8 days before B -band maximum. This makes it one of the earliest high-resolution spectra obtained of any SN Ia (a high-resolution spectrum of SN2011fe taken 1.5 days after explosion was presented in Nugent et al. 2011). Two follow-up spectra were obtained bracketing maximum light to cover the time frame at which changes due to photoionisation could be expected. Finally, two late spectra were taken on back-to-back nights to cover phases during which late-time absorption line variations have been observed in the past (e.g. SN 2006X, Patat et al. 2007). In the following, the two last spectra are treated as one epoch, since SNe Ia only evolve slowly at these late phases and an improved signal-to-noise ratio is achieved by coadding them.

3. NARROW ABSORPTION FEATURES

We searched all spectra for narrow absorption features in the rest frame of NGC 5643. While Ca II H&K lines

were immediately apparent in all spectra, Na I D absorption was only revealed after applying telluric line corrections. We searched, but did not detect CH and CH+ or any diffuse interstellar bands (DIBs) such as those identified in Sollerman et al. (2005). The frequently studied DIBs at $\lambda\lambda$ 5780 and 5797 fall in between the spectral arms (REDL and REDU) of the UVES spectra and K I lies outside the range of the instrument with the chosen set up.

Around $z = 0.004$, many telluric lines can make the identification of small Na I D absorption features difficult. In fact the telluric features in the spectra of the first two epochs were deeper and partially blended with the later detected Na I D in the host galaxy rest frame. In Table 1 the H₂O column determined from telluric line fitting is shown for reference. The Na I D features could be identified because,

- several features remained after telluric line correction at the redshift of NGC 5643,
- the features appeared as doublets with the separation and line ratios characteristic of Na I D,
- the features did not shift with the telluric lines between epochs,
- and the features appeared to have the same rest frame velocity as the deepest features of Ca II H&K.

The alignment of Na I D and Ca II H&K indicates that the detected features correspond to the same gas clouds situated along the line-of-sight of SN 2017cbv. The detected absorption lines are plotted in Figure 1 after normalising the continuum and correcting for telluric features. It can be seen that the Na I D and Ca II H&K features align well with one another.

We visually compared the profiles of each epoch for differences. In the profile of the most redshifted feature in Na I D2 (labeled VIII in Figure 1) a small peak appears. Notably, there is no feature at the corresponding wavelength in Na I D1. Although the pixels themselves are $\sim 3\sigma$ outliers from the scatter around the continuum, several comparable peaks in the continuum can be identified in this spectrum. For this reason we ignore the peak in the further analysis. No further significant differences could be visually identified between the epochs.

We have measured the pixel-for-pixel equivalent widths of the detected lines of each epoch. The measured total equivalent widths, which are presented in Table 2 and plotted in Figure 2 show no significant evolution across the period of the observations. The total Ca II H&K equivalent widths of the last epoch

MJD	UT Date	Exp. time (s)	Set-up	Epoch (days)	R ($\lambda/\delta\lambda$)	S/N [†]	H ₂ O column (mm)
57826.3	Mar. 14.3	1800	1.0" DIC1 390+580	-14.8	92,000	110	13.6 ± 0.3
57831.2	Mar. 19.2	2 × 1700	0.8" DIC1 390+580	-9.9	80,000	150	6.3 ± 0.1
57846.1	Apr. 03.1	2 × 2000	0.8" DIC1 390+580	5.0	64,000	210	1.4 ± 0.1
57923.2	Jun. 19.2	2 × 1700	0.8" DIC1 390+580	82.1	74,000	}110	1.2 ± 0.2
57924.0	Jun. 20.0	2 × 1700	0.8" DIC1 390+580	82.9	83,000		2.1 ± 0.2

[†]around 5900 Å

Table 1. The obtained UVES spectra. Epochs are with respect to the B -band maximum on MJD 57841.1 (Hosseinzadeh et al. 2017a). Resolutions are inferred from telluric line widths, which were computed with Molecfit along with the H₂O columns.

appear slightly lower but still consistent with the average values. Where possible, we also measured the equivalent widths of individual features or, if the lines are blended, we measured the equivalent widths across groups of features. In neither case significant trends could be identified.

We further fit Voigt profiles to the features, whereby we fit the profiles of each doublet of the same absorber simultaneously (Na I D1 with D2 and Ca II H with K). The fitted profiles are plotted in red over the spectra in Figure 1. We found that the Ca II H&K profiles can be fit well by nine individual components, while four of those match the profile of Na I D.

We studied the fitted column densities (N_X) and Doppler widths (b_X) of each feature without finding any significant trends, in agreement with the equivalent width measurements. Thus, there does not appear to be any changes to the absorbers over the observed period. In Table 3, the averaged Voigt profile parameters are presented, where the features are labeled the same way as in Figure 1. Given the similar Doppler shift of the features IV, V, VI and VIII, they probably correspond to the same gas clouds containing both Na I and Ca II gas.

Assuming the features originate from the same gas clouds, the profile widths should be the same in Na I D and Ca II H&K. In Table 3 it can be seen however, that the fitted widths of corresponding Na I and Ca II features do not all agree. While, b_{VIII} of Na I and Ca II agree well, b_{IV} , b_{V} and b_{VI} are in disagreement. Given that features IV, V and VI in Ca II H&K are blended with each other and that feature IV appears very broad, there could be several unresolved features in the profile causing the measurement discrepancy. Table 3 also contains the column density ratios $N_{\text{Ca II}}/N_{\text{Na I}}$ of the features detected in both lines. The large difference in ratios might indicate different levels of depletion in the clouds, although unresolved lines could also contribute to the differences.

4. DISCUSSION

In the absence of detectable variations, the photoionisation model of Borkowski et al. (2009) can be used to exclude radii at which significant amounts of gas are present. The distances excluded by a given absorber, depend on its ionisation energy and cross-section, as well as spectral energy distribution (SED) of the SN. The inner exclusion limit is defined by the distance within which any gas is ionised before the first spectrum is taken. Because SNe Ia peak in ultraviolet (UV) before maximum brightness in optical bands, it is crucial to obtain very early spectra (~ 2 weeks before maximum) to determine a strong limit (see Ferretti et al. 2016). The outer exclusion limit is defined by the distance beyond which there is negligible ionisation due to the low UV flux.

The non-detection of variations in both Na I D and Ca II H&K suggests that the gas clouds must be far from SN 2017cbv. The UV radiation should have caused detectable photoionisation of Na I within $R_{\text{Na I}}^{\text{outer}} \approx 2 \times 10^{19}$ cm and of Ca II within $R_{\text{Ca II}}^{\text{outer}} \approx 10^{17}$ cm, the farthest distances at which photoionisation can occur around SNe Ia. The absence of variations implies that the detected features must originate from gas farther from the supernova than these distances.

Assuming the SN Ia SED used in Ferretti et al. (2016), we determine the inner radius limits within which all Na I and Ca II gas must have been ionised before the first spectrum was taken. In the right panels of Figure 2 we show the modelled ionisation fraction of such CS gas clouds. We determined the inner limits of our sensitivity range to be $R_{\text{Na I}}^{\text{inner}} \approx 5 \times 10^{16}$ cm and $R_{\text{Ca II}}^{\text{inner}} \approx 6 \times 10^{14}$ cm. If the SED underestimates the UV flux, these radii will be larger. For example, if the supernova is fainter by 1 mag (factor 2.5) in UV, $R_{\text{Na I}}^{\text{inner}}$ is shifted out by $\sim 3 \times 10^{16}$ cm and $R_{\text{Ca II}}^{\text{inner}}$ by $\sim 4 \times 10^{14}$ cm. In conclusion, a CS gas shell that contains both detectable amounts of Na I and Ca II, must have been at $R < 10^{15}$ cm from the explosion to not be detected by our observations.

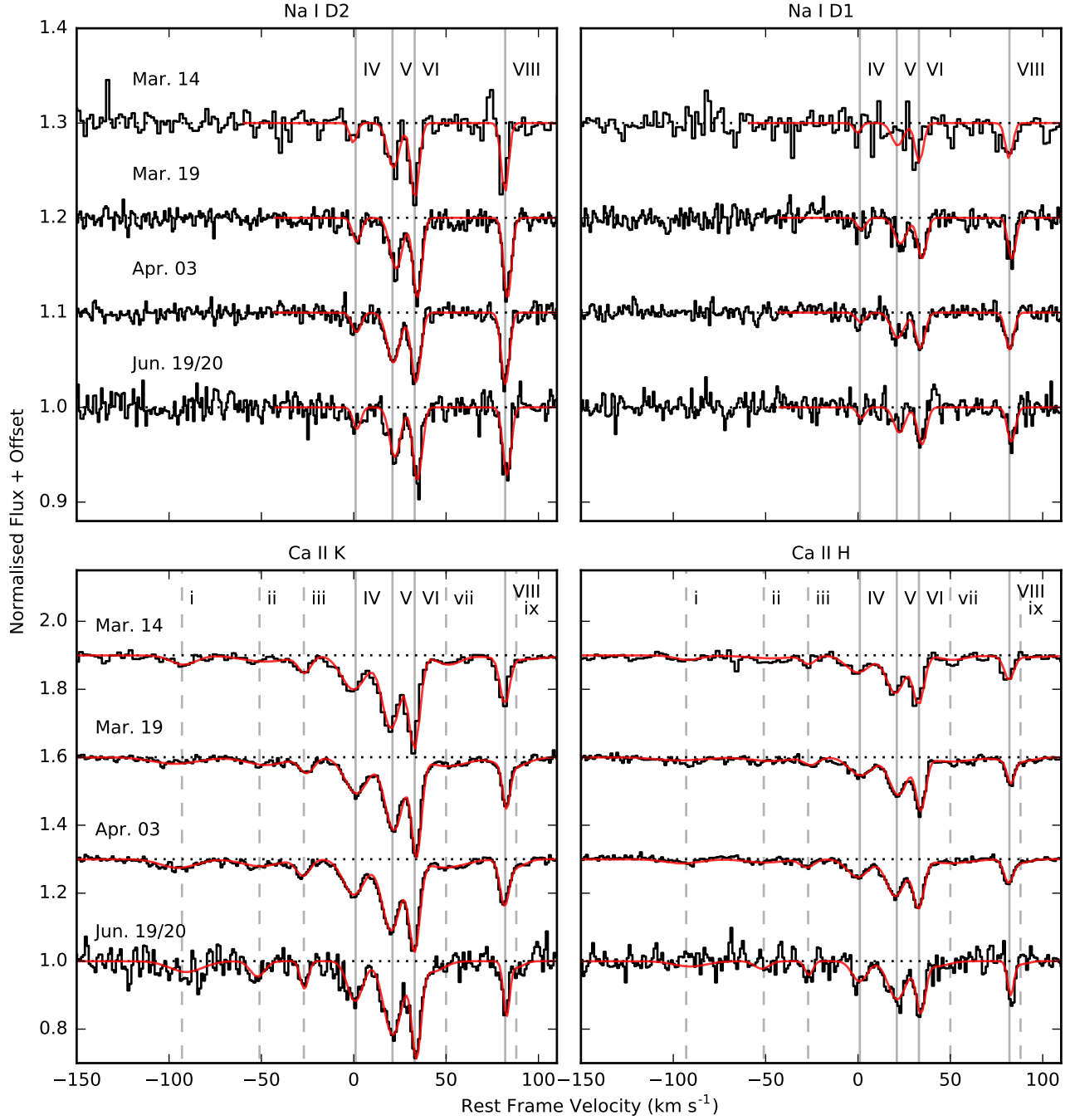


Figure 1. The detected Na I D and Ca II H&K features in velocity space of the host galaxy rest frame at $z = 0.004$. For clarity, the spectra, which are shown in black, have been normalised, offset and, in the case of Na I D, telluric line corrected. The fitted Voigt profiles are plotted in red and vertical lines indicate individual line components. Features present in both Na I D and Ca II H&K are marked with solid grey lines and labeled with capital Roman numerals, while features only detected in Ca II H&K with dashed grey lines and lower case Roman numerals.

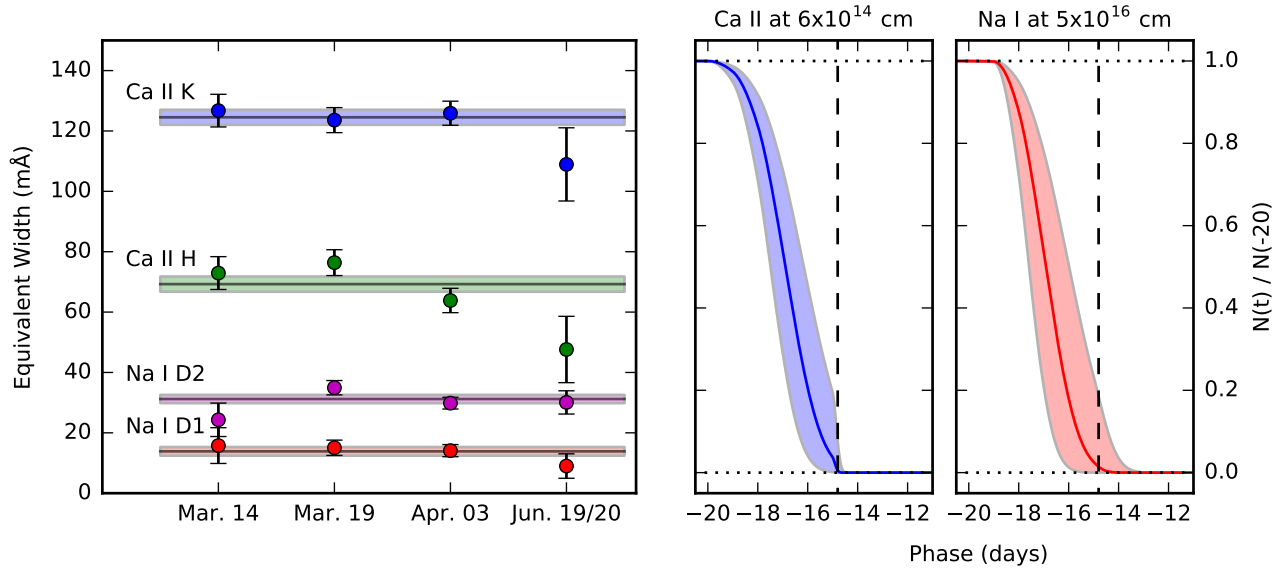


Figure 2. Left panel: Equivalent widths of Na I D and Ca II H&K. The weighted average equivalent widths of all epochs are plotted with horizontal lines with 1σ bands. No significant changes can be identified between the epochs. Right panels: Na I and Ca II ionisation curves at the inner exclusion limit. Any gas clouds closer to a SN Ia than those shown are ionised before an epoch of -14.8 days. The bands show the changes in the ionisation fraction if the UV flux of the SN varies by ± 1 mag (factor 2.5).

Obs. date	Epoch	Ca II K (mÅ)	Ca II H (mÅ)	Na I D2 (mÅ)	Na I D1 (mÅ)
Mar. 14	-14.8	$126. \pm 5.$	$73. \pm 5.$	$24. \pm 5.$	$16. \pm 5.$
Mar. 19	-9.9	$123. \pm 4.$	$76. \pm 4.$	$35. \pm 2.$	$15. \pm 2.$
Apr. 03	5.0	$125. \pm 3.$	$64. \pm 4.$	$30. \pm 1.$	$14. \pm 2.$
Jun. 19/20	83.	$108. \pm 12.$	$48. \pm 10.$	$30. \pm 3.$	$9. \pm 4.$

Table 2. Pixel-for-pixel equivalent widths of Na I D and Ca II H&K, measured across the full profile of the respective feature. Epochs are given with respect to B -band maximum.

Feature	v^\dagger (km s ⁻¹)	$z_{\text{Na I}}$	$\log_{10}\{N_{\text{Na I}}\}$ (cm ⁻²)	$b_{\text{Na I}}$ (km s ⁻¹)	$z_{\text{Ca II}}$	$\log_{10}\{N_{\text{Ca II}}\}$ (cm ⁻²)	$b_{\text{Ca II}}$ (km s ⁻¹)	$N_{\text{Ca II}}/N_{\text{Na I}}$
i	-91	–	–	–	0.003694(9)	10.92 ± 0.02	13.1 ± 0.8	–
ii	-52	–	–	–	0.003824(4)	10.88 ± 0.02	11.4 ± 1.0	–
iii	-27	–	–	–	0.003909(3)	10.80 ± 0.02	4.3 ± 0.3	–
IV	0	0.004005(3)	10.13 ± 0.03	2.1 ± 0.5	0.004001(2)	11.36 ± 0.01	7.9 ± 0.1	0.06
V	21	0.004074(1)	10.65 ± 0.01	3.9 ± 0.2	0.004069(1)	11.60 ± 0.01	6.2 ± 0.1	0.11
VI	34	0.004115(1)	10.70 ± 0.01	2.4 ± 0.2	0.004112(1)	11.49 ± 0.01	3.0 ± 0.1	0.16
vii	42	–	–	–	0.00414(3)	10.94 ± 0.03	12.3 ± 1.4	–
VIII	82	0.004277(1)	10.65 ± 0.01	1.8 ± 0.2	0.004275(2)	11.05 ± 0.02	1.7 ± 0.2	0.40
ix	87	–	–	–	0.00429(2)	10.87 ± 0.04	9.7 ± 1.4	–

[†] inferred from $z_{\text{Ca II}}$ with respect to $z = 0.004$

Table 3. Redshifts z_X , Column densities N_X and Doppler widths of b_X of the fitted Voigt profile components. The values are the average parameters obtained from fitting the profiles of each spectrum. Features are labeled the same way as in Figure 1, where capital roman numerals correspond to features detected in both Na I D and Ca II H&K, while the lower case roman numerals correspond to features only detected in Ca II H&K.

We further estimate upper column density limits for undetected Na I and Ca II gas in the respective excluded ranges. The limits are determined by identifying the lowest column density a feature can have to be detected in the first epoch. Since both Na I D and Ca II H&K are doublets, we can require an absorption feature to be identifiable in both profiles of a respective doublet for a detection. This implies that the lines must be identifiable in Na I D1 and Ca II H, the lines with the weaker oscillator strengths of their respective doublets. Supposing a feature with a Gaussian profile and a full-width-half-maximum of 0.1 Å, the column density would need to be more than $\log_{10}\{N_{\text{Na I}}^{\text{upper}} [\text{cm}^{-2}]\} = 10.4$ for a line to be identifiable above the noise in Na I D1. Notably, feature IV has a lower column density than this limit and is not detected in Na I D above the noise of the first epoch. Only in the later spectra, with higher signal-to-noise ratios, feature IV can be identified. Using the same criteria, a column density greater than $\log_{10}\{N_{\text{Ca II}}^{\text{upper}} [\text{cm}^{-2}]\} = 10.7$ is necessary to identify a feature in Ca II H in the first epoch.

The time series of high-resolution spectra suggest that the detected narrow absorption lines are at interstellar distances. Assuming similar ISM properties to our Milky Way, we can infer reddening from the Na I D equivalent width (Poznanski et al. 2012). The average total Na I D equivalent width of 45 ± 3 mÅ, suggests an $E(B - V) = 0.016 \pm 0.003$ mag. Thus, in agreement with Hosseinzadeh et al. (2017a), the inferred reddening is negligible.

Some SNe Ia have been shown to have unusually steep extinction curves (e.g. Amanullah et al. 2015). The pres-

ence of CS dust surrounding typical SNe Ia has been proposed as a possible explanation for steep extinction curves (Goobar 2008). To affect the extinction curve, the dust must be situated at distances closer than a few 10^{17} cm. It is thus of interest to determine whether any SNe Ia have dust in their CS environment. Supposing the dust is traced by Na I and Ca II gas, our observations are sensitive and exclude CS matter at distances of $\sim 10^{15}$ – 10^{19} cm from SN 2017cbv.

Hosseinzadeh et al. (2017a) suggest that the early blue excess of SN 2017cbv could be due to the supernova ejecta hitting a non-degenerate companion star (Kasen 2010) or CS matter surrounding the progenitor system (Piro & Morozova 2016). We will briefly address both of these scenarios in the context of our observations.

The early blue bump described in Hosseinzadeh et al. (2017a) could be compatible with a subgiant companion star with $\sim 20 R_\odot$, while no hydrogen emission is detected. A SD progenitor system, as the one proposed, must have reached the Chandrasekhar limit by mass transfer, which results in strong stellar winds during accretion. Models suggest that the outflows will excavate large low-density cavities with radii of $\sim 10^{19}$ – 10^{20} cm (Badenes et al. 2007) into the ISM. Similar cavities with smaller radii of a few 10^{17} cm have been suggested for DD He+C/O progenitors (Shen et al. 2013). Matter blown off the progenitors should collect at the edges of the cavities. Since photoionisation of Na I should occur up to distances of $\sim 2 \times 10^{19}$ cm from SNe Ia, the gas we detected in the spectra of SN 2017cbv must be located farther from the explosion than that distance. Thus, there is no evidence for CS gas at distances pre-

dicted by the models of Shen et al. (2013). However, a large cavity surrounding an SD progenitor such as those modelled in Badenes et al. (2007), is still consistent with the observations.

Another explanation for the early blue bump in the lightcurve can be due to CS matter close to the explosion (Piro & Morozova 2016). For this to occur, there must be $> 0.1 M_{\odot}$ at $\sim 10^{12}$ cm from the supernova, a radius at which the gas would be immediately ionised and hit by SN ejecta within an hour of explosion. Unfortunately, our observations are not sensitive to CS matter at these distances.

5. CONCLUSIONS

We have detected multiple Na I and Ca II gas clouds along the line-of-sight of SN 2017cbv, a SN Ia on the outskirts of its host galaxy NGC 5643. We have obtained multi-epoch high-resolution spectra with UVES starting at an early epoch of -14.8 days before maximum brightness. Due to the extensive time coverage of SN 2017cbv, we are sensitive to photoionisation occurring in gas clouds over a large part of the CS environment. We did not find any time-evolution in any of the detected narrow absorption features, which implies that no detectable Na I gas clouds could be present with $\sim 8 \times 10^{16} - 2 \times 10^{19}$ cm and Ca II within $\sim 10^{15} - 10^{17}$ cm from the explosion. The detected gas clouds must therefore be located further from SN 2017cbv than the outer limit, while any gas closer to the explosion than the inner limit would have been ionised before the first spectrum was obtained.

Hosseinzadeh et al. (2017a) suggest that an early blue excess in the lightcurve could be due to ejecta hitting a non-degenerate companion star in a SD progenitor system. They do however point out that a lack of a corresponding UV bump is in disagreement with the models of Kasen (2010) and propose several explanations for the discrepancy. A SD progenitor is predicted to have excavated large cavities with radii of $\sim 10^{19} - 10^{20}$ cm into the surrounding ISM and deposit matter at the edges (Badenes et al. 2007). Our observations thus exclude

the presence of significant amounts of matter from parts of this range. At the same time, no significant amounts of gas could have been at radii of a few 10^{17} cm, distances at which DD He+C/O progenitor models predict matter to be deposited (Shen et al. 2013). There are thus several interpretations for our observations, or combinations of them:

- There is no CS gas and the detected absorption features are part of the ISM of NGC 5643 and unrelated to SN 2017cbv.
- There is a CS cavity within the exclusion range, but the Na I and Ca II columns present at the edges are below the detection threshold of $\log_{10}\{N_{\text{Na I}}^{\text{upper}} [cm^{-2}]\} = 10.4$ and $\log_{10}\{N_{\text{Ca II}}^{\text{upper}} [cm^{-2}]\} = 10.7$.
- The outflowing matter of an SD progenitor system created a cavity larger than 2×10^{19} cm (consistent with models of Badenes et al. 2007) and at least some of the detected absorption features correspond to gas deposited at the edges.

Badenes et al. (2007) study Galactic SN Ia remnants and find no evidence of cavities surrounding them. The ejecta of these SNe appear to have run into normal ISM at radii smaller than the expected size of the cavities, suggesting that the progenitor systems did not sustain strong or long lasting outflows.

Our observations should add useful information to the open progenitor question of SN 2017cbv and SNe Ia in general. Late time observations, when SN 2017cbv reaches a nebular phase should provide further evidence, if there was a non-degenerate companion in the progenitor system. In the cases of SNe 2011fe and 2014J, nebular spectra provided strong evidence for the absence of a non-degenerate companion star (Lundqvist et al. 2015).

The authors acknowledge support from the Swedish Research Council (Vetenskapsrådet) and the Swedish National Space Board.

REFERENCES

- Amanullah, R., Johansson, J., Goobar, A., et al. 2015, MNRAS, 453, 3300
- Badenes, C., Hughes, J. P., Bravo, E., & Langer, N. 2007, ApJ, 662, 472
- Borkowski, K. J., Blondin, J. M., & Reynolds, S. P. 2009, ApJL, 699, L64
- Bulla, M., Goobar, A., Amanullah, R., Feindt, U., & Ferretti, R. 2017, ArXiv e-prints, arXiv:1707.00696
- Chomiuk, L., Soderberg, A. M., Chevalier, R. A., et al. 2016, ApJ, 821, 119
- Chugai, N. N. 2008, Astronomy Letters, 34, 389
- Dekker, H., D’Odorico, S., Kaufer, A., Delabre, B., & Kotzlowski, H. 2000, in Society of Photo-Optical Instrumentation Engineers (SPIE) Conference Series, Vol. 4008, Optical and IR Telescope Instrumentation and Detectors, ed. M. Iye & A. F. Moorwood, 534

- Dilday, B., Howell, D. A., Cenko, S. B., et al. 2012, *Science*, 337, 942
- Dong, S., Katz, B., Kushnir, D., & Prieto, J. L. 2015, *MNRAS*, 454, L61
- Ferretti, R., Amanullah, R., Goobar, A., et al. 2016, *A&A*, 592, A40
- Goobar, A. 2008, *ApJL*, 686, L103
- Goobar, A., & Leibundgut, B. 2011, *Annual Review of Nuclear and Particle Science*, 61, 251
- Graham, M. L., Valenti, S., Fulton, B. J., et al. 2015, *ApJ*, 801, 136
- Hoang, T. 2017, *ApJ*, 836, 13
- Hosseinzadeh, G., Sand, D. J., Valenti, S., et al. 2017a, *ArXiv e-prints*, arXiv:1706.08990
- Hosseinzadeh, G., Howell, D. A., Sand, D., et al. 2017b, *The Astronomer's Telegram*, No. 10164, 164
- Iben, Jr., I., & Tutukov, A. V. 1984, *ApJS*, 54, 335
- Johansson, J., Amanullah, R., & Goobar, A. 2013, *MNRAS*, 431, L43
- Johansson, J., Goobar, A., Kasliwal, M. M., et al. 2017, *MNRAS*, 466, 3442
- Kasen, D. 2010, *ApJ*, 708, 1025
- Kausch, W., Noll, S., Smette, A., et al. 2015, *A&A*, 576, A78
- Koribalski, B. S., Staveley-Smith, L., Kilborn, V. A., et al. 2004, *AJ*, 128, 16
- Kundu, E., Lundqvist, P., Pérez-Torres, M. A., Herrero-Illana, R., & Alberdi, A. 2017, *ApJ*, 842, 17
- Lundqvist, P., Nyholm, A., Taddia, F., et al. 2015, *A&A*, 577, A39
- Maeda, K., Tajitsu, A., Kawabata, K. S., et al. 2016, *ApJ*, 816, 57
- Maguire, K., Sullivan, M., Patat, F., et al. 2013, *MNRAS*, 436, 222
- Margutti, R., Parrent, J., Kamble, A., et al. 2014, *ApJ*, 790, 52
- Modigliani, A., Goldoni, P., Royer, F., et al. 2010, in *Proc. SPIE*, Vol. 7737, *Observatory Operations: Strategies, Processes, and Systems III*, 773728
- Nugent, P. E., Sullivan, M., Cenko, S. B., et al. 2011, *Nature*, 480, 344
- Patat, F., Cox, N. L. J., Parrent, J., & Branch, D. 2010, *A&A*, 514, A78
- Patat, F., Chandra, P., Chevalier, R., et al. 2007, *Science*, 317, 924
- Patat, F., Cordiner, M. A., Cox, N. L. J., et al. 2013, *A&A*, 549, A62
- Phillips, M. M., Simon, J. D., Morrell, N., et al. 2013, *ApJ*, 779, 38
- Piro, A. L., & Morozova, V. S. 2016, *ApJ*, 826, 96
- Poznanski, D., Prochaska, J. X., & Bloom, J. S. 2012, *MNRAS*, 426, 1465
- Raskin, C., & Kasen, D. 2013, *ApJ*, 772, 1
- Schlafly, E. F., & Finkbeiner, D. P. 2011, *ApJ*, 737, 103
- Shen, K. J., Guillochon, J., & Foley, R. J. 2013, *ApJL*, 770, L35
- Simon, J. D., Gal-Yam, A., Gnat, O., et al. 2009, *ApJ*, 702, 1157
- Smette, A., Sana, H., Noll, S., et al. 2015, *A&A*, 576, A77
- Sollerman, J., Cox, N., Mattila, S., et al. 2005, *A&A*, 429, 559
- Sternberg, A., Gal-Yam, A., Simon, J. D., et al. 2011, *Science*, 333, 856
- . 2014, *MNRAS*, 443, 1849
- Tartaglia, L., Sand, D., Wyatt, S., et al. 2017, *The Astronomer's Telegram*, No. 10158, 158
- Webbink, R. F. 1984, *ApJ*, 277, 355
- Whelan, J., & Iben, Jr., I. 1973, *ApJ*, 186, 1007